Dynamical Mechanical Analysis and Curing Analysis of Fouling Release Coatings and Components

ARTICLE *in* MACROMOLECULAR SYMPOSIA · OCTOBER 2006

DOI: 10.1002/masy.200651039

5 AUTHORS, INCLUDING:

John Texter
Eastern Michigan University
232 PUBLICATIONS **2,142**
CITATIONS

Dynamical Mechanical Analysis and Curing Analysis of Fouling Release Coatings and Components

Ted Provder,[1] *Shyam Malliprakash,*[1,2] *Sarjak Hemantkumar Amin,*[1,2] *Atheer Majid,*[1,2] *John Texter*[*1,2]

Summary: A commercially available fouling release (adsorbed foulants removed by shear flow) coating based on poly(dimethylsiloxane) and a commercial marine epoxy primer have been analyzed by diffusing wave spectroscopy and by thermal and dynamical mechanical methods. Diffusing wave spectroscopy reveals 7–9 distinct relaxation intervals over short (minutes) to long (20 hour) time scales. Several junctures of these intervals are shown to correlate with mechanically determined film formation parameters, such as set to touch times, tack free times, and dry through times. Thickness series of coatings made by casting illustrate similarities and distinct differences between the epoxy primer and poly(dimethylsiloxane)-based fouling release coating formulations. Several low temperature β transitions are resolved in the fouling release coatings in addition the α (T_g) transition in both formulations. A scaling analysis of the thickness series data shows that both the primer and the top coat exhibit a negative exponent for thickness; −0.77 for the epoxy; −1.2 for the top coat. Stress-strain experiments reveal further significant difference between these two types of elastomers. The elastic modulus for the epoxy is 1000-fold higher than for the topcoat. A small elastic modulus is thought to be key in the successful functioning of fouling release coatings. Analyses of substrate effects (wire mesh, fiberglass braid) and of coating or loading levels on dynamical mechanical properties, in comparison with thickness series of thin films are presented. The woven braid offers the advantage that it can be loaded more easily than can wire mesh substrates. The negative exponents show that thinner coatings may be more mechanically resilient than thicker coatings, as the ability to store and dissipate mechanical energy decreases as thickness increases.

Keywords: alpha transition; beta transition; coating; diffusing wave spectroscopy; DMA; dynamical mechanical analysis; elastomers; epoxy resin; fouling release; poly(dimethyl siloxane) resin; resin curing; speckle rate; stress-strain; thickness effects

Introduction

The physicochemical analysis of fouling release coating formulations for boating and shipping subsurface bottom coats is of high current interest as public and governmental pressures increase to replace biocidal-emitting antifouling coating formulations with environmentally benign fouling release formulations.[1,2] Fouling release coating formulations are being focused on low surface energy formulations and formulations that have a low solid (Young's) modulus. While numerous types of low surface energy polymers are being investigated, such as perfluoropolymers,[3–6] polysiloxanes,[7–10] and perfluorosiloxanes,[7,11,12] the only formulations currently commercially available are based upon poly(dimethylsiloxane). The primary objective

[1] Coatings Research Institute, Eastern Michigan University, Ypsilanti, MI 48197, USA
E-mail: jtexter@emich.edu
[2] School of Engineering Technology, Eastern Michigan University, Ypsilanti, MI 48197, USA

of fouling release coatings is to proffer low adhesion energies to biofilm-forming organisms, so that when the vessel moves, the hydrodynamic shear forces cause any adhering organisms to shear off.

This characterization study focuses on a thermomechanical analysis of a commercially available poly(dimethylsiloxane) fouling release formulation, and as well upon a commercially available marine epoxy primer. The mechanical properties so obtained will be useful in benchmarking other formulations being developed.

Experimental

The polymeric-based liquid coating formulations used in this study are commercially available and were obtained from marine supply stores. The epoxy primer was a two-part formulation and comprised approximately 55% by weight VOC. It also contained a mixture of particulates as pigments, including titania, amorphous silica, and nepheline syenite. The fouling release top coat bottom paint was a three part formulation and comprised approximately 28% by weight VOC. This fouling release formulation is based on poly(dimethylsiloxane) and contained titania as light scattering pigment.

Thermal analyses were conducted using a TA Instruments (New Castle, Delaware) Model Q800 Dynamical Mechanical Analyzer and a TA Instruments Q500 Thermogravimetric Analyzer (TGA). DMA studies were done at various temperatures, using liquid nitrogen as a coolant and were generally done at 1 Hz with single cantilever, thin film, and shear clamps.

Adaptive speckle imaging interferometry (ASII) of diffusing wave spectroscopy (DWS) was done with a single-beam prototype HORUS system provided by Formulaction (l'Union, France).[13] Short range motions of suspended particulates and polymeric random coils perturb the frequency of the incident laser beam in exact analogy to quasi-elastic light scattering.[14] These perturbations are on the order of the Brownian motion velocity of the scattering entities (pigments, polymers). The back scattered radiation produces a speckle image resulting from interfering backscattered waves. The dynamics of the fluctuations in these speckle images are retrieved by spatial correlation analysis, and the calculated decorrelation time, T (for the autocorrelation function to drop to 1/e of its initial value), provides the speckle rate (= 1/T). Proprietary sampling is done over many orders of magnitude in time to produce a plot of speckle rate as a function of time. Other descriptions of speckle rate analysis from DWS in back-scattering geometry[15,16] and in transmission geometry[14,17,18] have been given.

A modified B-K mechanical recorder (Model DT-BK-3, Paul N. Gardner Co., Inc., Pompano Beach, Florida) was used to measure set to touch through dry hard times according to ASTM D-5895-03 for evaluating drying or curing during film formation of organic coatings. The recorder was modified by using only one $12'' \times 7''$ glass plate instead of a series of $12'' \times 1''$ glass strips. A modified Bird applicator with 3 to 4 mils nominal wet film thickness was used to make draw downs for each formulation. The set to touch time (STT) time is the time at which the stylus first leaves a persistent visible wake; the tack free time (TFT) is the time at which this visible wake becomes intermittent; the dry hard time (DHT) is the time at which this intermittent wake becomes a scratch; the dry through time (DTT) is the time at which this scratch disappears.

This study will also examine some alternative approaches to studying coatings. Besides examining thin films ranging in thickness from fractions of a mm to several mm, we report results obtained where wire mesh and fiberglass braid were used to support liquid coating samples. Thin films ranging in thickness from 0.18 mm to 3.6 mm were obtained by casting in molds machined into a Teflon block. A cutter just under 13 mm in diameter was used to machine, at constant depth, rectangular molds about 31 mm long

(plus the semicircular ends). Wire mesh fabricated with 400 wires per inch was obtained from the Cleveland Wire Cloth and Manufacturing Company (Cleveland, Ohio)

Results and Discussion

The liquid coating formulations were prepared at room temperature and then dried at 25 °C in TGA isothermal scans. These gravimetric drying curves were consistent with the theoretical % solids, but overall were featureless, and gave no obvious mechanistic insight. The drying curves so obtained were fitted to the equation

$$w(t) = w_s(1 - e^{-t/\tau}) + e^{-t/\tau}$$

Where $w(t)$ is the fractional weight remaining at time t, w_s is the fractional weight of solids, and τ is the drying time constant. Time constants of 45 min and 30 min were obtained, respectively, for the epoxy and poly(dimethylsiloxane) liquid coatings.

The ASII speckle rate data as a function of time for the epoxy primer at room temperature ($25.2 \pm 1\,^{\circ}C$) and ambient humidity ($\langle rh \rangle = 18 \pm 5\%$) are illustrated in Fig. 1 over the first 20 hours of ambient cure. The semi-logarithmic representation is particularly useful, since wherever straight-line behavior is identified, one can infer an exponential decay process predominates. Early time behavior over the first 45 min of ambient curing is illustrated in the inset, where the upper curve presents Log Rate/Hz data and the lower curve depicts the weight loss data from the TGA analysis.

The early time speckle rate behavior decreases three orders of magnitude in the first 30 seconds, during which time the VOC evaporation has resulted in a weight loss of

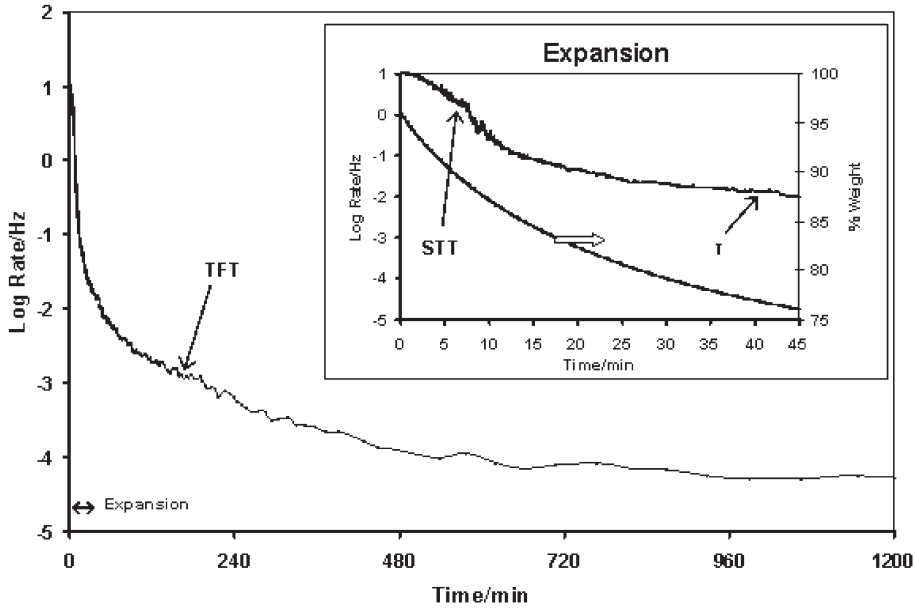

Figure 1.
Adaptive speckle imaging interferometry of diffusing wave dynamics during drying (curing) of epoxy resin at room temperature ($25.2 \pm 1\,^{\circ}C$). The inset (upper) illustrates the ASII response over the first 45 min and the simple weight loss curve (lower) obtained from parallel TGA measurements. The decay constant obtained from the TGA data is illustrated on the ASII curve in the inset. Also illustrated are the set to touch time (STT) and tack free time (TFT) obtained from parallel mechanical recorder experiments.

20%. The inset suggests the existence of four mechanistic regimes during the first 45 min, and the set to touch time (STT) appears to occur in between the first two at about 7 min. The TGA VOC evaporation decay constant, τ (44 min), appears within the ''fourth'' exponential decay interval. The intervals from 90 to 300 min, 300 to 660 min, and from 720 min on appear to be additional single-exponential decay intervals. Clearly, this collection of six to seven semi-logarithmic intervals presents an interpretive challenge in deciphering the detailed mechanism of drying and curing of this epoxy-based primer. The tack free time (TFT) appears in the middle of this 90–300 min interval. The pot life of this primer is about 5 h at these ambient conditions. This time period corresponds to the juncture of two intervals, but the corresponding rates above and below this juncture at 300 min are not very different.

Comparable TGA and ASII data for the fouling release top coat based on poly(dimethylsiloxane) are illustrated in Fig. 2. The upper curve in the inset portrays six speckle rate intervals, and several additional intervals, 290–330 min, 330–600 min, and 600 min onward, are apparent. Again, the TGA drying time constant occurs near the beginning of the third speckle rate interval, and at about this time, 30 min, nearly half the VOC has evaporated. In this system the set to touch time (STT) occurs towards the end of the fourth speckle rate interval, the tack free time (TFT) occurs at the juncture of the sixth and seventh interval, and the dry hard time (DHT) occurs at the beginning of the eighth interval. The pot life at ambient is approximately 3 h for this formulation, so it is reasonably to conclude that cross-linking kinetics are steadily increasing over the 120–240 minute interval, and we may surmise that the sudden decrease in speckle rate at 240 min is a result of network formation undergoing rapid acceleration. While a large decrease in speckle rate is

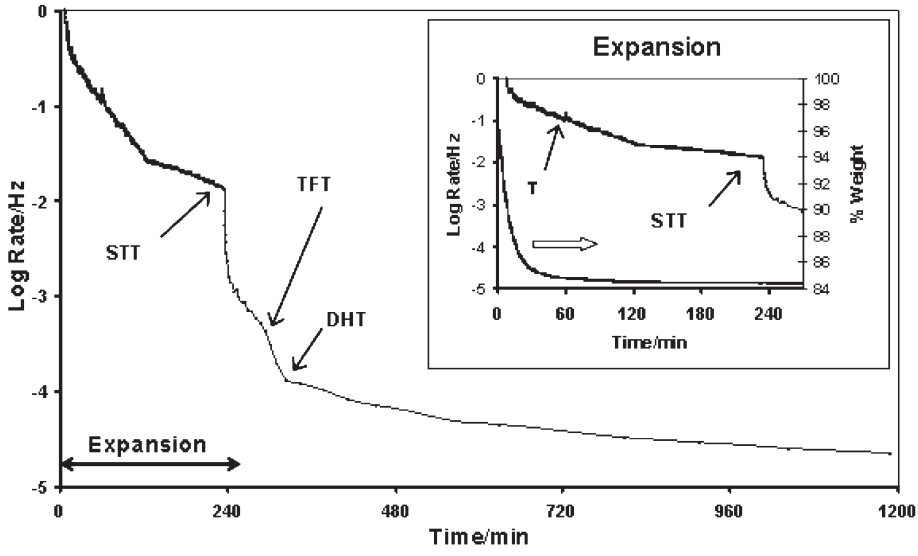

Figure 2.
Adaptive speckle imaging interferometry of diffusing wave dynamics during drying (curing) of fouling release poly(dimethylsiloxane) resin at room temperature ($25.2 \pm 1\,^{\circ}C$). The inset (upper) illustrates the ASII response over the first 300 min and the simple weight loss curve (lower) obtained from parallel TGA measurements. The decay constant obtained from the TGA data is illustrated on the ASII curve in the inset at about 30 min. Also illustrated are the set to touch time (STT), tack free time (TFT), and dry hard time (DHT) obtained from parallel mechanical recorder experiments.

observed in this system, somewhat after the predicted pot life, the actual speckle rate of about 1 mHz is the same as found in the primer data of Fig. 1 after the 5 hour pot life (300 min).

It appears that the kinetics of film formation are resolved over many different time scales by ASII. The challenge that confronts us is to assign these varied relaxation processes to the actual mechanistic physicochemical events occurring in the film. These events appear bounded from the short time end by VOC evaporation and pigment packing events and from the long time end by polymeric crosslinking and relaxation events. A question by Professor Bernhard Wolf in the oral delivery of this paper highlights the desirability of being able to do these ASII measurements as a function of temperature. When that is done, we will be able to experimentally derive activation energies for the processes occurring during the various exponential decay intervals.

Some mechanistic processes that may kinetically dominate over different time intervals during drying and curing of coatings include (1) solvent evaporation; (2) solvent evaporation hindered by closely packed droplets or particles; (3) cross linking; (4) further hardening due to evaporation of low molecular weight components.[14] Back scattered speckle rate DWS studies of colloidal systems drying suggest the existence of three time constants for particle motion.[19] One of these relaxations (the most rapid) is from (5) motion of particles in their Brownian "cage". Another is a more collective motion resulting from drying that causes compaction of the particles, but occurs (6) prior to reaching a critical concentration. Finally, another time constant attends the glass transition where (7) collective particle motion exhibits a yield stress.

A recent discussion has in a cogent way illustrated the interplay between drying and cross-linking.[20,21] These competitive processes are also convoluted with polymer falling through its glass transition.

The long-time speckle rate behavior in both Figs. 1 and 2 suggests curing has not reached completion after the nearly 24 hours of the experiments. In fact, the manufacturers suggest the epoxy primer be given two days to cure before over coating and seven days to cure before immersing in water. In Fig. 3 we see that at the relatively

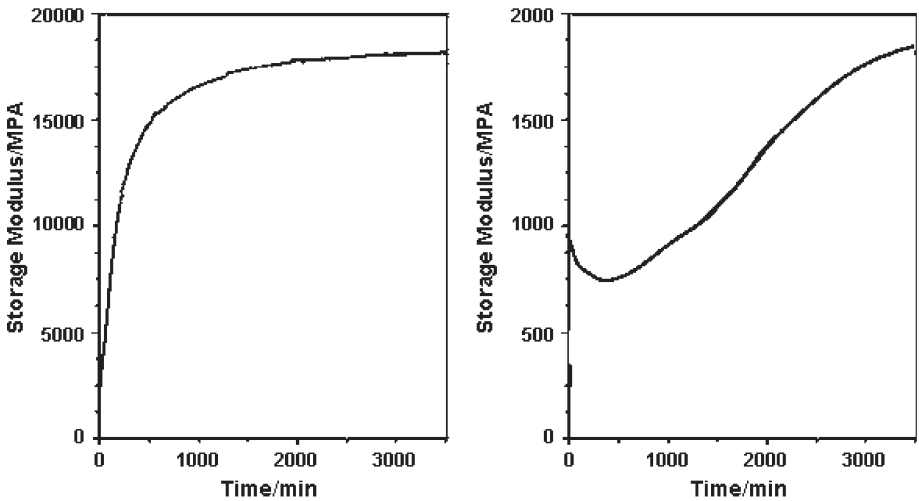

Figure 3.
Isothermal (50 °C) storage moduli for (left) epoxy primer and (right) poly(dimethylsiloxane) fouling release coating measured by single cantilever clamp at a frequency of 1 Hz. Each sample was spread on baked fiberglass braid.

high temperature of 50 °C, the isothermal cure storage modulus does no appear to have reached its asymptote after 3500 min (~2.5 days). At 20–25 °C we would expect such curing to take perhaps up to four times longer.

In these isothermal cure experiments the fiberglass braid substrates, cut to a length of about 30 mm and prebaked at 350 °C to pyrolyze any organic sizing, were loaded with 17.3 mg (cured weight) on 162.3 mg braid in the case of epoxy primer and 22.6 mg (cured weight) on 133.5 mg braid in the case of the fouling release poly(dimethylsiloxane) formulation.. The loaded braid was then placed in the two clamps in single cantilever mode, and the storage modulus was measured as a function of time at 50 °C. The braid by itself exhibits a storage modulus in the range of 300–400 MPa in single cantilever measurements over the range of 0–140 °C. The very high moduli illustrated in Fig. 3 are undoubtedly related to the high surface to volume ratio obtained by loading porous braid with the liquid coating formulations.

An alternative approach to supported coating samples is to cast coatings at various thicknesses, cure them, and then examine their thermomechanical properties. In Fig. 4 we illustrate thickness series for both the epoxy primer (left) and the poly(dimethylsiloxane) fouling release topcoat (right). For the epoxy coating series the castings (in Teflon block) were cured for a week at room temperature and then heated at 50 °C for several hours. The epoxy results in Fig. 4 (left) for the storage modulus were obtained using a single cantilever clamp at 1 Hz, and we see that the magnitude of the storage modulus dramatically decreases as sample thickness increases to several mm. Similarly, we see that the corresponding loss modulus decreases with increasing thickness, and further that the α (T_g) transition steadily shifts to lower temperature with increasing thickness.

Similar results are illustrated in Fig. 4 (right) for the poly(dimethylsiloxane) formulation. Samples were cured for a week at room temperature and then heated at 50 °C for several hours before measurements were made. However, these samples were too fragile to survive single cantilever clamp measurements, and they fractured shortly after the beginning of such experi-

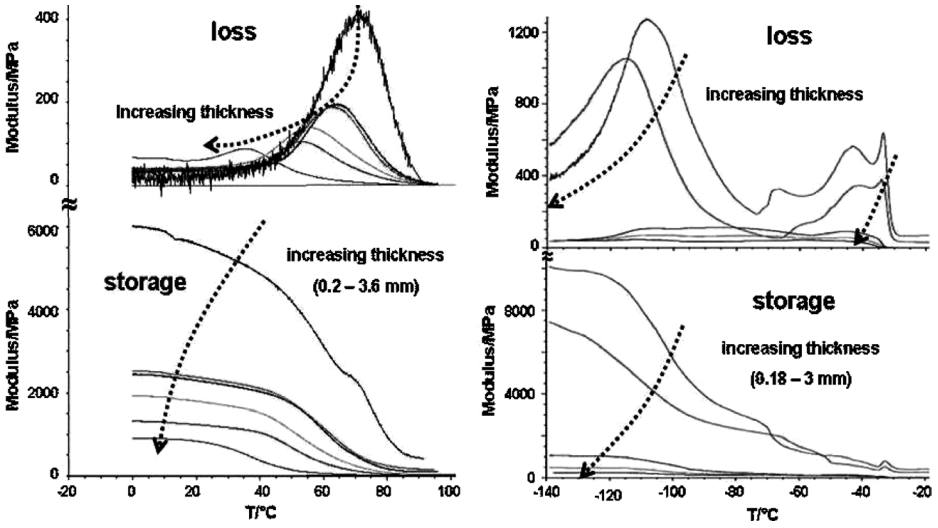

Figure 4.
Loss and storage moduli for (left) epoxy primer cast thickness series of samples measured by single cantilever clamp in DMA and (right) poly(dimethylsiloxane) fouling release cast thickness series of samples measured by shear clamp in DMA. The illustrated curves are for thicknesses (left) of 0.22, 0.43, 0.47, 0.98, 1.85, and 3.6 mm and (right) 0.18, 0.22, 1.1, 2.1, and 3.3 mm.

ments. As an alternative, the samples were examined using a shear clamp at 1 Hz. These measurements did not fracture the samples, and the results are those shown in Fig. 4 (right). Again we see the storage modulus dramatically decrease as the sample thickness increases. In this case, significant storage moduli are only observed below the α transition, between −140 and −20 °C. The effects of increasing sample thickness on the loss modulus are even more dramatic. The loss modulus of the thin samples exhibits three β transition below the α transition. As thickness increases, the relatively sharp α and first two β transitions shift to lower temperature and become very broad. The most intense β transition decreases in magnitude and shifts out of view with increasing thickness.

While the epoxy primer and the poly(dimethylsiloxane) topcoat exhibit some gross similarities, their behaviors differ in some key respects. Most importantly they differ in their moduli as a function of temperature. Note that the storage and loss moduli illustrated in Fig. 4 (right) are shifted by about 120 °C downward relative to the epoxy results. This shift means that under service conditions of −10 to 30 °C, the fouling release topcoat will be much, much softer than the underlying epoxy primer. In addition, the three β transitions in the fouling release composition suggest the cured coating exhibits a more complex array of mechanical energy dissipation mechanisms than in the epoxy primer.

The most significant unifying similarity between the two materials is the dramatic decrease in moduli with increasing thickness. This decrease has significant ramifications for in service wear and durability. Increasing thickness results in lower storage moduli and lower loss moduli. These trends imply that a coating's ability to withstand impact or shock may dramatically change with thickness, and that thinner coatings may in fact be much more durable than thicker coatings! Thicker coatings can reversibly store less energy and dissipate less energy, necessitating transformation of the excess mechanical energy in some untoward pathway (cracking, delamination, defect enlargement, severing chemical bonds, etc.).

The scaling behavior of these storage modulus results (Fig. 4) with sample thickness was examined by plotting the logarithm of the maximum storage modulus against the logarithm of the sample thickness. These results are illustrated in Fig. 5 for both the epoxy primer and poly(dimethylsiloxane) topcoat. In view of the results of Fig. 4, the thickness exponent is negative in both cases, −0.77 for the epoxy primer and −1.2 for the poly(dimethylsiloxane).

Stress-strain curves are illustrated in Fig. 6 for both the epoxy primer (left) and the fouling release poly(dimethylsiloxane)

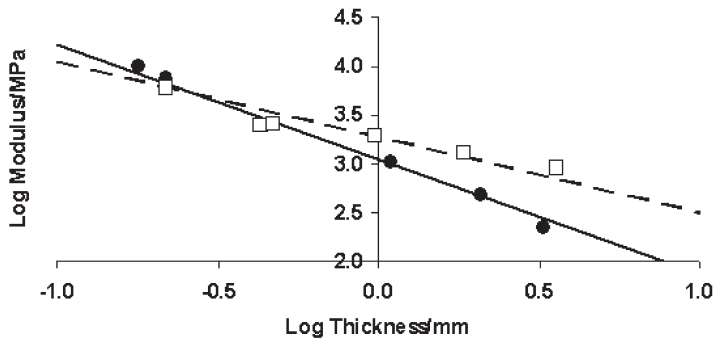

Figure 5.
Log Storage Modulus vs Log sample thickness for epoxy (●; at 0 °C) and poly(dimethylsiloxane) (□; at −130 °C) thickness series samples illustrated in Fig. 4. The exponent for the epoxy series is −0.77 and the exponent for the poly(dimethylsiloxane) series is −1.2.

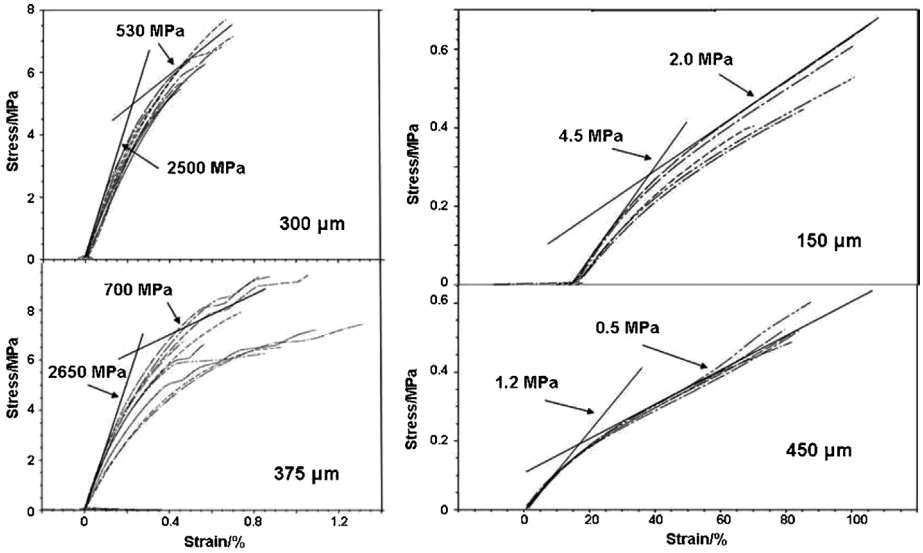

Figure 6.
Stress-strain plots for (left) epoxy primer cast samples and (right) poly(dimethylsiloxane) fouling release cast samples, all measured using a thin film clamp in DMA at 25 °C.

topcoat (right). These measurements were done with the DMA using a thin film clamp for cast samples. Samples for analysis were generally excised using a 5 mm-wide cutter, and lengths of about 20 mm.

The epoxy primer samples of both thicknesses, utilizing PTFE particles, exhibits a very high elastic modulus. The highest levels are illustrated with tangents, and are of the order of 2.5–2.7 GPa. The lower bounds are in the range of 1.5–1.7 GPa. The slightly thicker sample exhibits a slightly higher modulus, which is contrary to expectation in view of the negative thickness exponent illustrated earlier. However, this discrepancy can in part be accounted for by slightly different curing conditions for the two samples. The elastic modulus is competitive with values obtained using carbon nanotubes and nano-alumina as reinforcing fillers with comparable strain values at failure.[22] This low stretch ability with strains of 1.005–1.01 is markedly less than the 7% strain obtained with epoxies set without fillers.[23] This low strain at failure is indicative of a fairly high cross-linking density.[24]

The behavior illustrated in Fig. 6 (right) for the poly(dimethylsiloxane)-based coating is markedly different. The elastic modulus 1–5 MPa is in the range commonly encountered in siloxane rubbers,[25–27] and is comparable to Hansen's measurement of silica-filled cross-linked poly(dimethylsiloxane).[28] Unfilled PDMS stretches to a strain of 600%.[29] The elasticity is a hundred-fold greater than that of the epoxy, but markedly less than that obtained in the absence of fillers. The low elastic modulus accounts for the materials fragility in single cantilever experiments. However, it is believed that such a low value is conducive to fouling release behavior.

The thickness behavior for the fouling release topcoat in Fig. 6 (right) again underscores the impact of coating thickness on mechanical properties. The thinner sample can store more mechanical energy than the one that is three times as thick. We do not have a definitive explanation yet for this phenomenon, and unpublished results suggest that the negative exponent scaling observed in this study is not universal. However, some of these effects must be due

to coupling between polymeric surface states and bulk states. Increasing surface T_g and decreasing bulk T_g with decreasing thickness has been reported [30], and there is increasing interest in such phenomena wherein there are large surface to volume effects and interface effects [31]. An appropriate analysis of such phenomena requires a detailed free energy balancing of the surface and bulk physical states, that are very sensitive to molecular structure, packing, and interfacial effects.

A preliminary comparison of substrate effects on DMA measurements is illustrated in Fig. 7, where wire mesh and fiberglass braid substrates are compared. Both substrates appear to be useful. A possible advantage of the fiberglass braid is that the extent of loading can be varied over a wider dynamic range, since the *de facto* porosity of the braid facilitates liquid coating uptake. The absolute magnitudes of the moduli measured cannot be accounted for as of yet by any theory, but the qualitative variations of storage and loss moduli with temperature appear in reasonable agreement with results obtained from thin samples obtained by casting.

The depiction of epoxy curing in the upper left portion of Fig. 7 shows the initial commencement of curing from the liquid state as modulus slowly increases as temperature approaches 150 °C at 2°/min. The temperature is then quickly lowered and the modulus increases, passing through the T_g, to the high temperature asymptotic value. The steady increase in the low temperature modulus shows that each excursion to high temperature results in incrementally more curing. This sample was loaded with 257 mg epoxy on wire mesh 13.2 mm × 22.0 mm (45.6 mg). Similar effects are shown in the lower left portion of Fig. 7, where temperature increases and decreases were ramped at 2°/min, and 10.2 mg coating (cured weight) was spread over a piece of fiberglass braid weighing 157.7 mg. There is hysteresis in both the storage and loss moduli, and the incremental changes with further curing are small but steady.

The fouling release topcoat curing depicted on the right in Fig. 7 shows hysteresis in the cyclical scans (2°/min) in the braid-supported sample (lower). This sample was prepared by coating 80.9 mg of

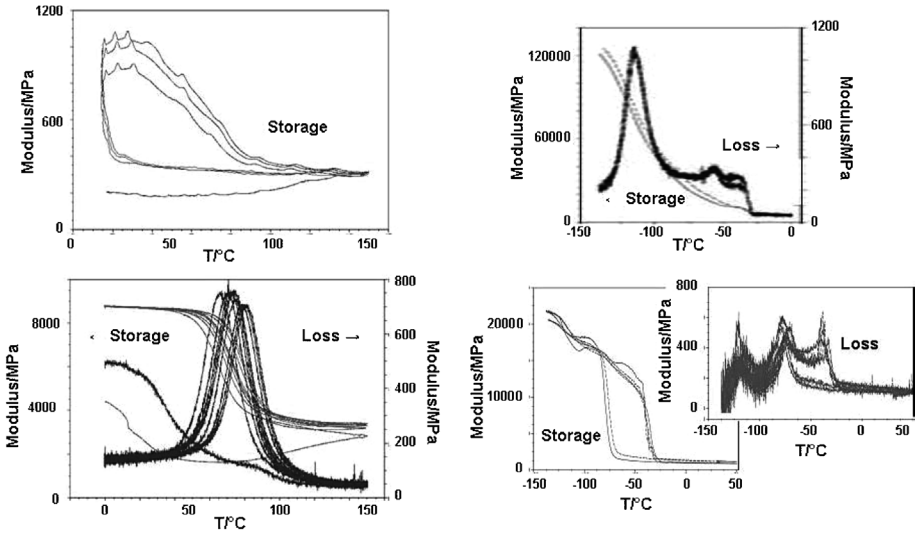

Figure 7.
Comparison of epoxy primer (left) and poly(dimethylsiloxane) fouling release (right) coatings evaluated on wire mesh (top) and fiberglass braid (bottom) substrates in DMA measurements at 1 Hz using a single cantilever clamp.

coating (cured weight) on fiberglass braid weighing 146.2 mg. The wire mesh supported sample in the upper portion was prepared with 28.2 mg of coating (prior to curing) on 80.8 mg of wire mesh.

Conclusions

ASII speckle rate studies and isothermal storage modulus experiments on braid-supported coatings illustrate that both the epoxy primer and poly(dimethylsiloxane) fouling release topcoat formulations require a week or more at ambient conditions to fully cure. The speckle rate analyses reveal 7-9 exponential decay mechanistic regimes during ambient curing, whereas simple gravimetric drying provides only a single time constant. This difference suggests ASII will become an important analytical tool for analyzing film formation in the near future. Several mechanically generated film formation parameters were found to occur at or close to the juncture of ASII decay regimes.

Thickness series for each formulation exhibited storage and loss moduli that decrease with increasing sample thickness, and α transitions (and β transitions in the case of poly(dimethylsiloxane)) shift to lower temperature with increasing sample thickness. A scaling analysis of the maximal storage modulus yielded negative exponents of order -1 for the thickness for both types of disparate coating formulations.

The stress-strain studies yielded elastic (Young's) moduli in conformity with values reported for similar materials. The poly(-dimethylsiloxane) formulation is much more rubbery than the epoxy primer, although both are elastomers. The effects of fillers on elasticity have a dramatic effect on decreasing the strain at failure.

Both wire mesh and fiberglass braid substrates appear useful for examining liquid coating formulations. The braid can advantageously be loaded more heavily with liquid coating because of its *de facto* porosity.

The negative exponent scaling observed for both formulations and illustrated by decreasing moduli with increasing sample thickness reveals a significant relationship between mechanical properties and coating thickness. Thinner samples may be more durable, because of their ability to reversibly store and dissipate more energy! This observation suggests thickness optimization of coatings may be an important design feature, with a view toward protecting against mechanical deformations and perturbations.

Acknowledgements: The molds for casting samples for the thickness series were kindly prepared by Professor Erik Lokensgard. This work was supported by the United States Office of Naval Research through grant award No. N00014-04-1-0763.

[1] R. F. Brady, *Defence Sci. J.* **2005**, *55*, 75.
[2] M. Berglin, K. J. Wynne, P. Gatenholm, *J. Colloid Interface Sci.* **2003**, 257, 381.
[3] J. C. Yarbrough, J. P. Rolland, J. M. DeSimone, M. E. Callow, J. A. Finlay, J. A. Callow, *Macromolecules* **2006**, 39, 2521.
[4] J. Wang, G. Mao, C. K. Ober, E. J. Kramer, *Macromolecules* **1997**, 30, 1906.
[5] D. Gan, A. Mueller, K. L. Wooley, *J. Polym. Sci. Part A: Polym. Chem.* **2003**, 41, 3531.
[6] C. S. Gudipati, C. M. Greenlief, J. A. Johnson, P. Prayongpan, K. L. Wooley, *J. Polym. Sci. Part A: Polym. Chem.* **2004**, 42, 6193.
[7] M. A. Grunlan, N. S. Lee, F. Mansfield, E. Kus, J. A. Finlay, J. A. Callow, M. E. Callow, W. P. Weber, *J. Polym. Sci. A: Polym. Chem.* **2006**, 8, 2551.
[8] G. W. J. Swain, M. P. Schultz, *Biofouling* **1996**, 10, 187.
[9] J. K. Pike, T. Ho, K. J. Wynne, *Chem. Mater.* **1996**, 8, 856.
[10] J. G. Kohl, I. L. Singer, *Prog. Org. Coat.* **1999**, 36, 15.
[11] E. Johnston, S. Bullock, J. Uilk, P. Gatenholm, K. J. Wynne, *Macromolecules* **1999**, 32, 8173.
[12] M. A. Grunlan, N. S. Lee, G. Cai, T. Gädda, J. M. Mabry, F. Mansfeld, E. Kus, D. E. Wendt, G. L. Kowalke, J. A. Finlay, J. A. Callow, M. E. Callow, W. P. Weber, *Chem. Mater.* **2004**, 16, 2433.
[13] HORUS Advanced Drying Analysis, http://www.horus-drying.com/UK_horus/home.htm, accessed 27 May 2006.
[14] A. J. Breugem, F. Bouchama, G. J. M. Koper, *Surf. Coatings Intl. B. Coatings Trans.*, **2005**, 88, 135.
[15] R. Bandyopadhyay, A. S. Gittings, S. S. Suh, P. K. Dixon, D. J. Durian, *Rev. Sci. Inst.*, **2005**, 76, 093110-1.

[16] A. Federico, G.H. Kaufmann, G.E. Galizzi, H. Rabal, M. Trivi, R. Arizaga, *Opt. Commun.* **2006**, 260, 493.
[17] P. Zakharov, F. Cardinaux, F. Scheffold, Phys. Rev. E, **2006**, 73, 011413; DOI: 10.1103/PhysRevE.73.011413
[18] F. Schosseler, S. Kaloun, M. Skouri, J. P. Munch, Phys. Rev. E, **2006**, 73, 021401; DOI: 10.1103/PhysRevE.73.021401.
[19] T. Marital, C. Beauvais, P. Hébraud, and F. Lequeux, *Eur. Phys. J. E*, **2004**, 14, 287.
[20] M. Dušková-Smrčlová, K. Dušek, *J. Mat. Sci.* **2002**, 37, 4733.
[21] K. Dušek, M. Dušková-Smrčková, *Prog. Poly. Sci.* **2000**, 25, 1215.
[22] Nanocomposites; Matrix: Epoxy, Rensselaer Polytechnic Institute, Troy, NY, 2003-2004; http://www.academy.rpi.edu/projects/nano/nanocomposites/start.php, downloaded May 31, 2006.
[23] T. E. Tay, H. G. Ang, V. PI. W. Shim, *Comp. Structures* **2005**, 33, 201.
[24] M. T. Rodrıguez, J.J. Gracenea, A.H. Kudamaa, J.J. Suay, *Prog. Org. Coatings* **2004**, 50, 62.
[25] K. D. Jamani, E. Harrington, H. J. Wilson, J. Oral Rehabil. **1989**, *16*, 241.
[26] J. F Lontz, J. W. Schweiger, A. W. Burger, Paper No. 890.: Modifying stress-strain profiles of polysiloxane elastomers for improved maxillofacial conformity, Annual Meeting of the International Association for Dental Research, Dental Materials Group, Atlanta, Georgia, March 21-24, 1974.
[27] W. J. O'Brien, Biomaterials Properties Database, University of Michigan, Ann Arbor, Michigan, 1997; http://www.lib.umich.edu/dentlib/Dental_tables/intro.html, downloaded May 31, 2006.
[28] D. E. Hansen, *Polymer* **2004**, 45, 1055.
[29] P. Wang, S. L. Wunder, *Polymer* **1997**, 38, 3417.
[30] C. J. Ellison, J. M. Torkelson, *Nature Materials* **2003**, 2, 695.
[31] Z. M. Ao, Q. Jiang, *Langmuir* **2006**, 22, 1241.

